Journal of Applied Polymer Science

Effects of maleic anhydride grafted polyethylene on rheological, thermal, and mechanical properties of ultra high molecular weight polyethylene/poly(ethylene glycol) blends

Shuai He, Hui He, Yingchun Li, Dongqing Wang
Department of Polymer Science and Engineering, College of Materials Science and Engineering, South China University of Technology, Guangzhou 510640, China
Correspondence to: H. He (E-mail: pshuihe@scut.edu.cn)

ABSTRACT: Ultra-high molecular weight polyethylene (UHMWPE) has gained considerable fame due to its excellent wear and mechanical properties, though the inferior processability has restricted its further extensive applications. In this study, a combination of UHMWPE and poly(ethylene glycol) (PEG) was considered based on the recent reports, and aiming to further exploit the potential of PEG that acts as processing aid, and also to obtain greater enhanced processability along with other properties, the effects of incorporating maleic anhydride grafted polyethylene (MAPE) was thoroughly investigated. Rheological tests revealed a further significant reduction in melt viscosity of UHMWPE/PEG blends after MAPE introduced, showing a potential of better processability, while the flexural strength and toughness of UHMWPE blends experienced a satisfying increase without any obvious compromises in other mechanical properties. A slight improvement of thermal stability in UHMWPE ternary blends along with an increase of vicat softening temperature were characterized by thermal tests, while the crystallinity of UHMWPE was diminished after the introduction of MAPE. Morphology analysis indicated that better dispersion and decreased size of PEG particles were achieved in UHMWPE matrix when MAPE was incorporated, which confirmed the improved interfacial interactions and other reinforcements obtained in UHMWPE/PEG/MAPE blends. © 2015 Wiley Periodicals, Inc. J. Appl. Polym. Sci. **2015**, *132*, 42701.

KEYWORDS: blends; compatibilization; morphology; polyolefins; surfaces and interfaces

Received 13 April 2015; accepted 4 July 2015
DOI: 10.1002/app.42701

INTRODUCTION

In recent years, an increasing attention has been drawn to ultra high molecular weight polyethylene (UHMWPE) as a result of its outstanding toughness, high abrasion resistance, superior wear strength in bearing surfaces and biocompatibility for total joint replacement.[1] UHMWPE, composed of entirely hydrogen and carbon atoms, has been widely used in various applications ranging from gears, liners, unlubricated bearings and seals[2] to total joints for orthoplastics in the area of biomechanics.[3] However, due to the extremely high molecular weight, UHMWPE can hardly be processed using conventional methods. Even above its melting temperature, UHMWPE still possesses a high level of melt viscosity, and thus the mainstream thermoplastic processing techniques like extrusion and injection molding cannot be utilized for UHMWPE with the exception of compression molding and ram extrusion,[4,5] which largely restricts its efficiency of mass production. Factors such as molecular weight and its distribution, the composition and the compatibility of the blends, and the processing methods and the corresponding parameters are found to be responsible for the processability of UHMWPE. Hence, for the purpose of achieving the processing of UHMWPE with conventional techniques, investigations into those factors are obviously necessary and also of great practical and scientific interests.

Numerous work and research have been done regarding the melt viscosity reduction of UHMWPE. Commonly used practice, such as blending conventional polyethylene (LDPE, HDPE) and polypropylene (PP) with UHMWPE under various processing conditions,[6–14] introducing a small quantity of processing aids like polyethylene wax, fluoroelastomer, liquid crystalline polymer and stearates,[15,16] incorporating nanosized inorganic fillers,[17] are comprehensively studied. To some extent, these approaches are imperfect which means the improved processability may bring dramatic decrease in other properties of UHMWPE, like mechanical performances, wear resistance, etc.[18] Adding a small amount of HDPE into UHMWPE presents unsatisfying effects for the processability, making it incapable for general processing methods, though UHMWPE/HDPE blends do show an enhancement regarding thermal stability and ductility due to their decent miscibility.[19] Also, Huilin Li *et al.*[20] reported the introduction of a small quantity of PP (10 wt %)

could significantly improve the processability of UHMWPE with a remarkable reduction of its melt viscosity, whereas the mechanical properties of the UHMWPE/PP blends witness an evident decrease as a consequence of their inferior compatibility. In terms of processing aids, although they do behave effectively in reducing the viscosity of UHMWPE, there is usually a small saturation level for them.[18] Recently researchers have found an effective approach to make it possible for UHMWPE being properly extruded without the sacrifice of its essential properties that previously possessed. They discovered that incorporating a very small amount of Poly(ethylene glycol) (PEG) can surprisingly improve the extrudability of UHMWPE, though slight loss of mechanical strength is unavoidable due to the polarity differences between hydroxyl-rich PEG and methylene-rich UHMWPE.[21] PEG could migrate to the die wall and the skin of UHMWPE product during the extruding operations,[22] and this phenomenon is responsible for the limited enhancement as the surface lubrication is much less effective than interior disentanglement. Hence, in order to further develop the effectiveness of PEG, the addition of HDPE, PP, and other common fillers like diatomite and glass bead has found helpful to the greater melt viscosity reduction of UHMWPE.[18,22]

In order to further develop the potential of PEG, enhancing its compatibility with UHMWPE is essential, and also this is the major objective of this study. Therefore, in this research, a novel approach was designed to strengthen the interfacial interactions between PEG and UHMWPE. A very small quantity of maleic anhydride-grafted polyethylene (MAPE) was introduced into the UHMWPE/PEG blends, and theoretically, MAPE can bridge the polarity gap between UHMWPE and PEG as MAPE possesses both polar and non-polar functional groups, which is also the reason that MAPE is widely used in plastic composites industry as a coupling agent.[23–27] Hopefully, through the coupling function of MAPE, the processability and compatibility of UHMWPE/PEG can be evidently enhanced to meet our expectations.

EXPERIMENTAL

Materials

- UHMWPE (powder, melting point: 145°C; molecular weight = 1.7×10^6 g/mol) was kindly provided by Beijing No. 2 Auxiliary Agent Factory, Beijing, China with a density of 0.90 g/cm^3.
- PEG (PEG6000, melting temperature: 64−66°C; molecular weight = 6000−8000 g/mol) was supported by Aoke Chemical Limited, Liaoyang, China with a density of 1.27 g/cm^3.
- MAPE (melting point: 120°C; grafting rate: 1.0%) was purchased from Kingfa Scientific and Technological with a melt flow index (MFI) of 1.4−2.0 g/10 min (190°C, 2.16 kg load).

Blends Preparation

The same amount of PEG and MAPE were mechanically mixed before melt processing. They were ground into powder and blended evenly using a Universal pulverizer for 2 min. Then, the mixed additives were blended with UHMWPE per a precise weight proportion. The formula was fixed as UHMWPE:PEG:MAPE = 100 : 3: x (x varied from 1 to 5, per hundred resin, phr) and used in all the following experiments. Another formula UHMWPE : PEG = 100 : 3 was also adopted as a reference group, and they were evenly mixed before processing.

The above two groups were fed into a twin-screw extruder (Polylab OS 16/40, Germany) at 230°C, respectively, and the extrudates were cut into granules for further operations. Then, the pure UHMWPE powder, UHMWPE/PEG, and UHMWPE/PEG/MAPE granules were respectively compressed with a model for 10 min in the Hot Press Machine (XLB-D vulcanizing press, Zhejiang Hongtu machinery factory) at 210°C and 20 MPa, and the product was slowly cooled with pressure to obtain a sheet. The sheet was then placed at least 24 h before further processing. Lastly, the sheet was cut by a Dumbbell System Prototype (TF-2062, Tianfa Test Machinery) according to the ISO standard to gain testing bars. Bars for Izod impact test were processed to obtain a notch per the standard.

Mechanical Properties Tests

Testing bars for the tensile, flexural, and Izod notched impact tests were prepared according to ISO 527:1993, ISO 178:1993, and ISO 180:1993 on Shimadzu AG-1, Instron 4465, and Zwick Pendulum 5113.300, respectively. The mechanical tests were performed at room temperature and the data were collected based on the average of five samples. Also, the strain−stress curves were tracked during tensile tests.

Rheological Properties Tests

During the extrusion, the die pressure of different groups was recorded at varied screw rotation speed. Rheological measurements were performed on a capillary rheometer (RHEO - TESTER 1000, L-893) at 210°C. The range of apparent shear rates was between 100 and 4000 s^{-1}. The rheological data were calculated directly on the rheometer with the consideration of Bagley correction.

Thermal Properties Tests

Vicat softening temperature tests was conducted on an Italian HDT-VICAT Thermal Deformation/VICAT Temperature tester, 50 N loaded, and the heating rate was 120°C/h. The temperature when the needle was pressed 1 mm into the sample was recorded.

Thermogravimetry Analysis (TGA) tests were performed on a Q5000 thermal gravimetric analyzer, TA Instrument U.S to determine thermal degradation behavior of the blends. The heating rate was 10°C per minute from 30°C to 700°C under nitrogen protection, and the TGA curves of the blends were recorded. The initial decomposition temperature when the weight loss reaches 5% and the peak decomposition temperature are recorded as $T_{5\%}$ and T_p.

Differential Scanning Calorimetry (DSC) tests were carried out on an American DSCAQ20 automatic differential scanning calorimeter. The heating and cooling rate were both 10°C/min, and the operating temperature range was 30°C−200°C. This whole procedure was under the protection of nitrogen, and the gas flow was 50 mL/min. DSC curves of heating and cooling scans

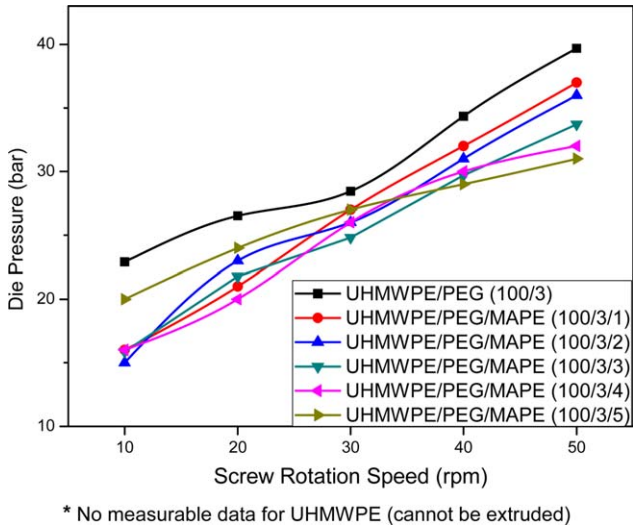

Figure 1. The die pressure of UHMWPE blends at varied screw rotation speed. [Color figure can be viewed in the online issue, which is available at wileyonlinelibrary.com.]

of each sample were tracked and their peak temperature were then recorded, respectively, referred to as T_{Mp} and T_{Cp}. The half-peak width values ($W_{C1/2}$) of each cooling curves were calculated to determine crystallization rate. The relative crystallinity, X_c, was calculated according to the following equation:

$$X_c = (\Delta H_{exp}/\Delta H^\circ) \times 100\% \quad (1)$$

where ΔH_{exp} is the melting enthalpy of UHMWPE calculated by TA Universal Analysis according to the corresponding melting curves, and ΔH° is the melting enthalpy of totally crystallized polyethylene, which is assumed to be 293 J/g.[28]

Scanning Electron Microscopy

The Bio-Rad SEM spray system was employed to spray the fracture surfaces of each sample with platinum. The Netherlands FEI, Quanta 200 environmental SEM was then utilized to observe the morphological characteristics. The fracture surfaces were obtained through several procedures. First, samples were frozen by liquid nitrogen to become brittle, and then sudden impact was used to break them. The smooth fracture surfaces were then obtained and utilized to conduct the SEM characterization.

Fourier Transform Infrared Spectroscopy (FTIR)

FTIR spectra of different samples were recorded in transmission mode on a Bruker Vertex 70 FTIR spectrometer at a spectral resolution of 4 cm^{-1} and 32 scans.

RESULTS AND DISCUSSION

Rheological Properties of UHMWPE Blends

Figure 1 shows the die pressure of the extruder when processing UHMWPE blends at different screw rotation speed. Pure UHMWPE cannot be extruded, and thus there is no measurable data. Adding a small amount of PEG (3 phr) enables UHMWPE to be processed by the extruder, and the die pressure rises with the increasing screw rotation speed. Incorporating MAPE into the UHMWPE/PEG blends can decrease the die pressure of the extruder at every rotation speed level, which indicates better extruding behavior, though adding different proportion of MAPE does not show much significant difference in terms of die pressure reduction. The large drop in die pressure provides substantial potential for increasing production rate by speeding up screw rotation and reducing energy cost.[22]

The results of capillary rheometer measurement are presented in Figure 2. The increased shear rate during the capillary test of UHMWPE causes severe pressure vibration, and no steady rheological data could be obtained above the shear rate of 115 s^{-1}. Introducing PEG into UHMWPE remarkably reduces the apparent viscosity, up to 36.4% of the virgin UHMWPE at the shear rate of 115 s^{-1}, and the extruding process during the test becomes steadier. The incorporation of MAPE further decreases the apparent viscosity of UHMWPE blends, and the maximum viscosity reduction in percentage is 40.9% at the shear rate of 230 s^{-1} with 3 phr MAPE. Decreased melt viscosity after adding PEG and MAPE offers UHMWPE better processability, and also gives UHMWPE the capability of being processed by common extruder. UHMWPE possesses distinctively high molecular weight, and thus its molecular chains are fairly long and huge. These chains tend to entangle with each other spontaneously, and they hardly stretch or flow at the temperature even higher than its melting point.[29–31] The function of PEG acted as lubricant greatly reduces the melt viscosity of UHMWPE, but its potential is still not fully exploited as PEG particles tend to migrate to the surface of the product during extruding due to the inferior compatibility. Hence, involving MAPE moderates this condition as it owns both polar groups and polyethylene segments that possess great compatibility with PEG and UHMWPE, improving the dispersion of PEG particles. In general, better dispersed PEG further lubricates UHMWPE segments and thus enhances their fluidity.

As different amount of MAPE does not bring significant changes concerning melt viscosity, which is the main objective of this research, the addition of 3 phr MAPE was used to be tested in the following experiments.

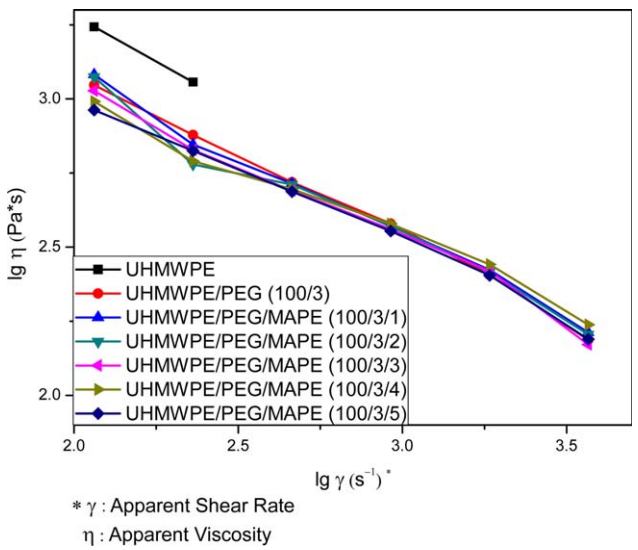

Figure 2. Apparent flow curves of UHMWPE blends. [Color figure can be viewed in the online issue, which is available at wileyonlinelibrary.com.]

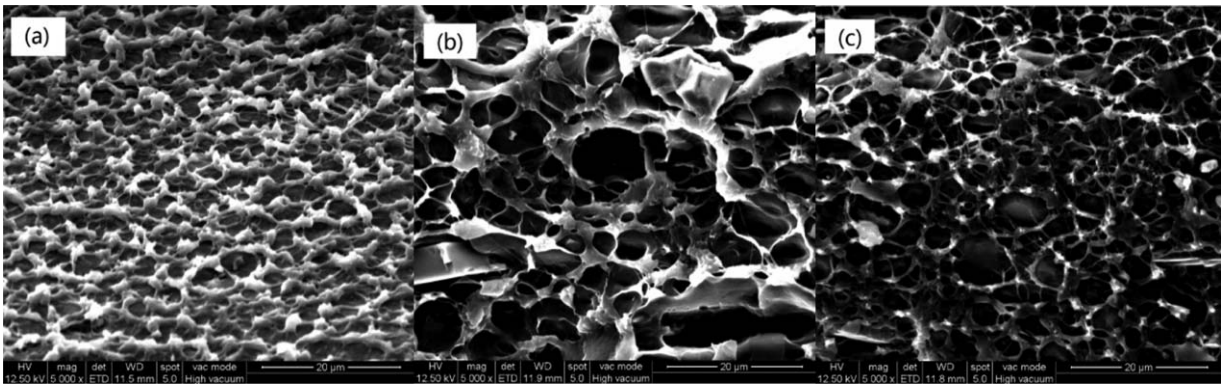

Figure 3. SEM micrographs of UHMWPE blends (×5000): (a) UHMWPE, (b) UHMWPE/PEG (100/3), (c) UHMWPE/PEG/MAPE (100/3/3).

Functioning Mechanism of MAPE on UHMWPE/PEG Blends

The actual effects of MAPE on UHMWPE/PEG blends and their detailed mechanism are proposed in this section. Figure 3 shows the interior morphology of three different materials, photographed by SEM.

The fractured surface of UHMWPE presents uniform morphology composed of millions of rod-like structure, and these tiny "rods" connects with each other, offering UHMWPE superior toughness. Adding a small quantity of PEG dramatically transforms the interior morphology of virgin UHMWPE, and a vast number of voids can be observed. Undoubtedly, this distinct structure is caused by PEG particles, which are barely compatible with UHMWPE matrix. PEG particles disperse in the form of sphere, and they are directly dragged out when sudden impact applied. It is rather interesting to see the interior structure of UHMWPE/PEG blends being remarkably altered once again when MAPE incorporated. From Figure 3(c), the voids become much smaller and they disperse more evenly when comparing with UHMWPE/PEG. Hence, it is reasonable to assume that the addition of MAPE reduces the particle size of PEG and also increases the dispersion of those particles, and this phenomenon can be adopted to explain the enhanced processability and decreased melt viscosity of UHMWPE/PEG/MAPE ternary blends.

Figure 4 presents information regarding the interaction between MAPE and PEG, which can better explain the influence of the addition of MAPE/PEG on UHMWPE. Form Figure 4, it can be easily observed that the decomposition temperature of PEG and MAPE varies nearly 150°C, and when combining them, the decomposition temperature increases compared to PEG by around 100°C instead of showing two distinct weigh-losing stages, which means the interactions do exist between PEG and MAPE, and thus enables them to possess one decomposing stage. Therefore, the addition of MAPE and PEG has synergistic effects to UHMWPE matrix. On the other hand, Figure 5 presents FTIR spectra information of PEG, MAPE and MAPE/PEG blends. The transmittance peak located at 1756 cm^{-1} is attributed to the —C═O vibration of the maleic anhydride group, which existed in MAPE. It is obvious to notice that this transmittance peak disappears after blending PEG and MAPE, indicating that chemical reactions happened between the maleic anhydride group of MAPE and hydroxyl groups of PEG. This phenomenon suggests the potential functioning mechanism of MAPE/PEG blends in UHMWPE.

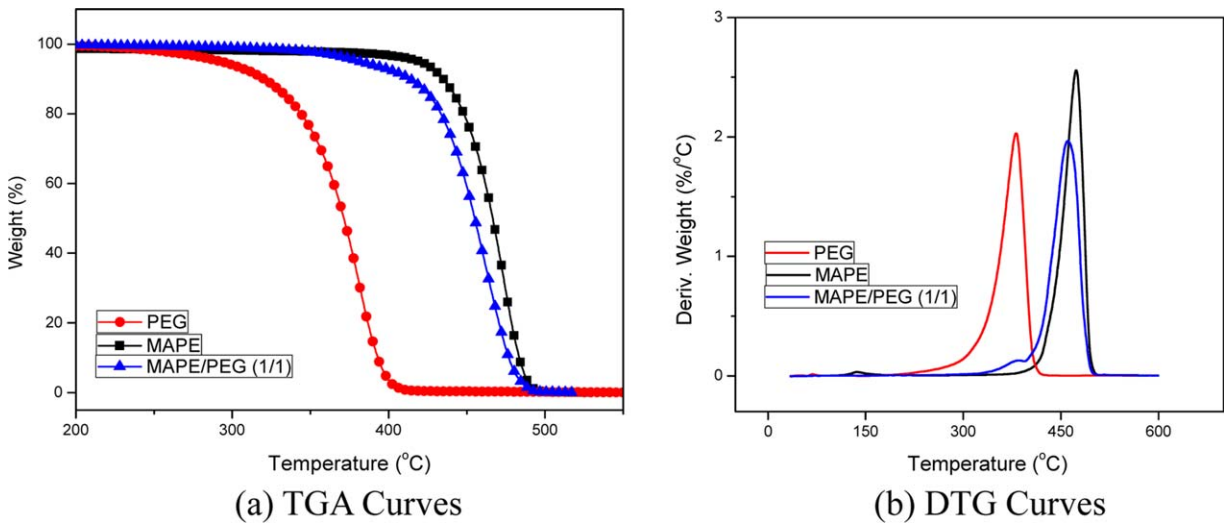

Figure 4. TGA curves of PEG, MAPE, and MAPE/PEG blends. (a) TGA curves (b) DTG curves. [Color figure can be viewed in the online issue, which is available at wileyonlinelibrary.com.]

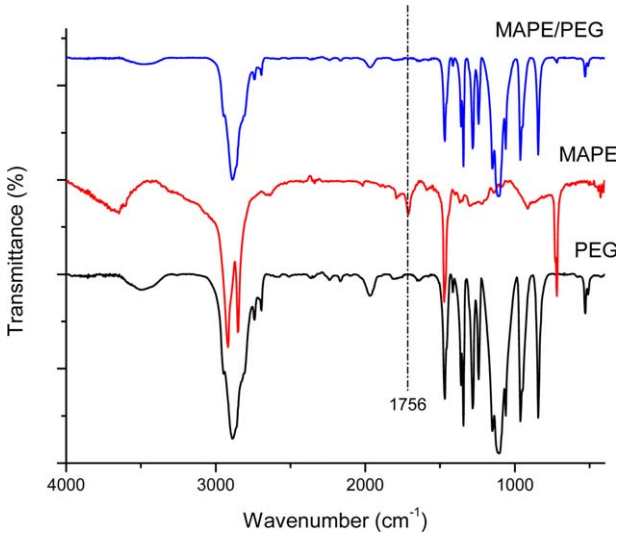

Figure 5. FTIR spectra of PEG, MAPE, and MAPE/PEG blends. [Color figure can be viewed in the online issue, which is available at wileyonlinelibrary.com.]

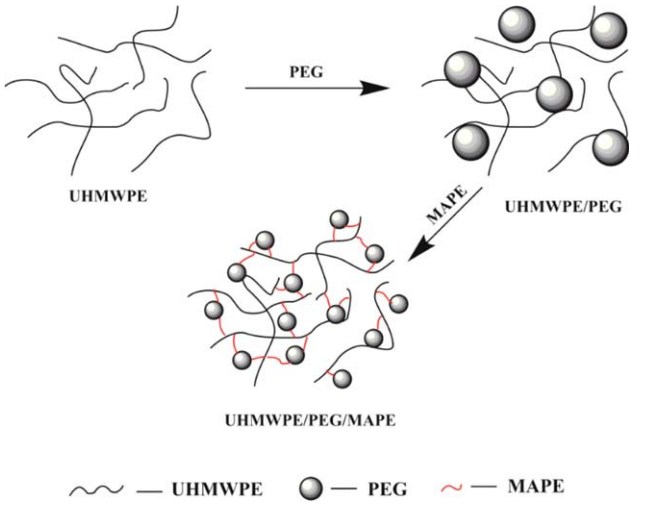

Figure 6. Schematic diagram of the effects of MAPE on UHMWPE/PEG blends. [Color figure can be viewed in the online issue, which is available at wileyonlinelibrary.com.]

The functioning mechanism of MAPE on UHMWPE/PEG blends is speculated as shown in Figure 6. The interior structure of UHMWPE consists of countless molecular chains that twist and entangle with each other, and they also crystallize to form a typical semi-crystalline polymer structure, though their degree of entanglement greatly exceeds the normal ones as a result of their extremely high molecular weight. Those unique characteristics make UHMWPE possess very high melt viscosity at a temperature even much higher than its melting point, and thus adding processing aids, like PEG, is necessary to improve the processability of UHMWPE. The addition of PEG makes a great contribution in lowering the melt viscosity of UHMWPE. It has already been reported that most PEG particles exist in the exterior zone of the product, and also PEG mainly located and play an important role in the amorphous region of the virgin UHMWPE matrix.[18] Although a certain level of decreased melt viscosity is achieved by adding PEG, there is still a great potential that has not been fully exploited for PEG particles. However, based on the results that have been received from the above experiments, it is reasonable to deduce that introducing MAPE further enhances the viscosity-lowering function of PEG. On the one hand, the particle size of PEG is greatly reduced and it disperses more uniformly after MAPE added. On the other hand, the inferior compatibility between UHMWPE and PEG as a result of their discrepancy in polarity is improved by the addition of MAPE. As MAPE consists of both polar groups and non-polar polyethylene groups, it has great compatibility with UHMWPE and PEG. Therefore, the interactions between MAPE and UHMWPE or PEG are fairly strong, and thus the interfacial bonding for the material as a whole is enhanced. Overall, the involvement of MAPE improves the interfacial interactions between UHMWPE and PEG as well as the dispersion of PEG particles in the matrix, and thus brings better processability and enhancements in other properties of the ternary blends.

Mechanical Properties of UHMWPE Blends

Table I presents the mechanical performances of different UHMWPE blends. The tensile strength of UHMWPE does not deteriorate much after PEG added, and the involvement of MAPE slightly improves the strength of the ternary blends. This is explainable, as PEG itself does not possess superior mechanical strength, and its addition will jeopardize the continuity of the matrix; therefore, the decrease of the tensile strength is within expectation. However, due to the inferior compatibility between PEG and UHMWPE, most PEG particles will migrate to the surface of the material,[32] and thus its deteriorating function regarding tensile strength is not obvious. Hence, the addition of MAPE will certainly exert little effects on the tensile strength as a result of the low strength that PEG pristinely has. In terms of flexural strength and flexural modulus, UHMWPE/PEG/MAPE blends clearly possess the highest figure when comparing with other groups. PEG particles played as foreign matter vastly disperse in UHMWPE, and this condition more or

Table I. Mechanical Properties of UHMWPE Blends

Samples	Tensile strength (MPa)	Flexural strength (MPa)	Flexural modulus (MPa)	Impact strength (KJ/m^2)	Elongation at break (%)
UHMWPE	20.3	25.3	880	91.9	640
UHMWPE/PEG (100/3)	20.0	25.6	928	92.8	560
UHMWPE/PEG/MAPE (100/3/3)	20.6	28.0	944	97.6	760

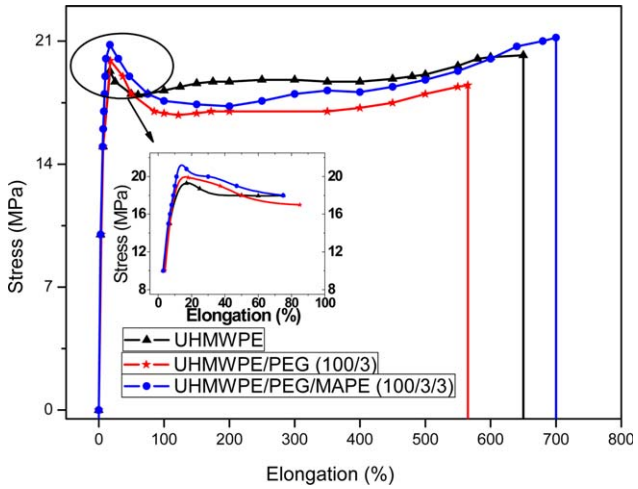

Figure 7. Stress-elongation curves of UHMWPE blends. [Color figure can be viewed in the online issue, which is available at wileyonlinelibrary.com.]

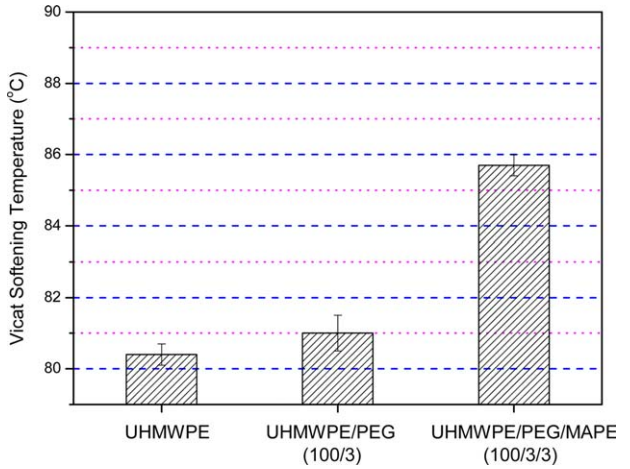

Figure 8. Vicat softening temperature of UHMWPE blends. [Color figure can be viewed in the online issue, which is available at wileyonlinelibrary.com.]

less causes numerous defects. Nevertheless, MAPE acted as a bridge connects PEG and UHMWPE, forming a more integrated structure,[33–35] and thus the ternary blends are capable of withstanding stronger forces from external and greater deformation. Hence, the improvement of the stiffness that reflected by flexural modulus is justified. Regarding impact strength, UHMWPE itself possesses a high level of toughness due to its distinct structure and behavior during deformation;[36,37] thus, its blends should have similar super toughness. It can be evidently observed from the table that the incorporation of MAPE enhances the capability of UHMWPE/PEG blends defending sudden impact, which indicates better toughness. The improved compatibility and continuity of the blends are responsible for the enhanced impact strength compared to UHMWPE/PEG. It is even more interesting that UHMWPE/PEG/MAPE (97.6 KJ/m^2) possesses greater toughness than virgin UHMWPE (91.9 KJ/m^2). It is proposed that the addition of PEG decreases the entanglement density of UHMWPE,[21] which means the molecular chains of UHMWPE obtain a chance to stretch themselves from aggregated groups. Thus, the improved mobility enables chain segments to shift and adjust against sudden shocks, and the movements of molecular chains can absorb greater amount of energy, yet the PEG particles will also act as stress concentration points impairing the toughness of the material. The roles of PEG are therefore becoming mutually opposite. However, the involvement of MAPE can just moderate the adverse function of PEG particles, making them closely connected with UHMWPE. This assumption can be partly confirmed by the improved impact strength of UHMWPE/PEG/MAPE blends.

Figure 7 demonstrates the tensile testing process of three materials, and the elongation versus stress curves shows the status of each group under stress. All these samples present similar trend, and firstly, the stress value is rising quickly along with the increasing elongation. Soon, the stress reaches a peak value, which is the yield strength, before it goes down to an extent, and then the stress value mildly grows until the sample breaks.

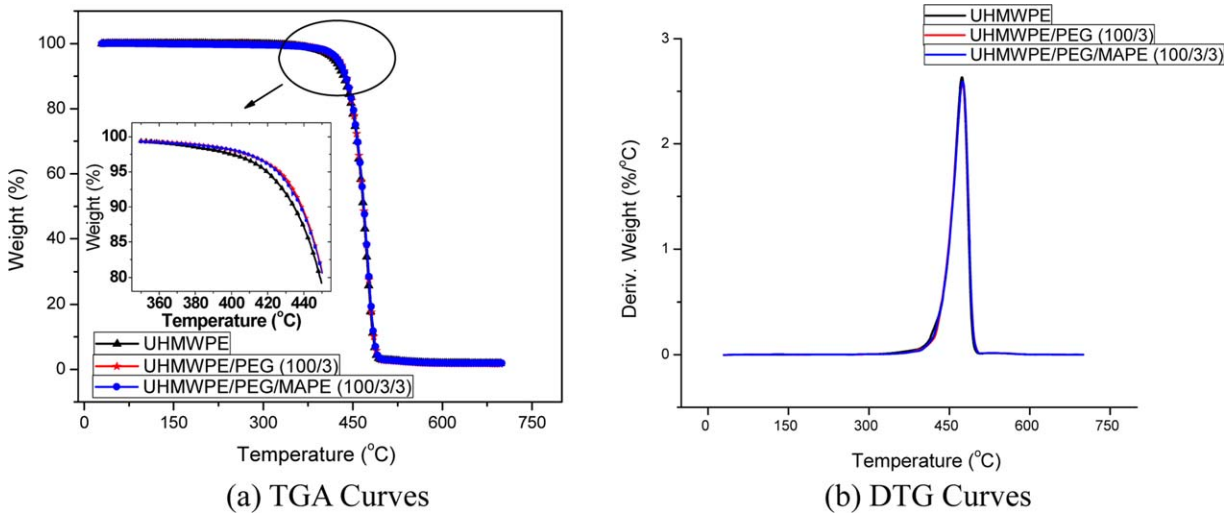

Figure 9. TGA curves of UHMWPE blends. (a) TGA curves (b) DTG curves. [Color figure can be viewed in the online issue, which is available at wileyonlinelibrary.com.]

Table II. TGA Data of UHMWPE Blends

Samples	UHMWPE	UHMWPE/PEG	UHMWPE/PEG/MAPE
$T_{5\%}$/°C	419.4	426.5	425.4
T_p/°C	474.3	473.6	475.0

Table III. Data Obtained from the DSC Scans of UHMWPE Blends

Samples	T_{Mp} (°C)	T_{Cp} (°C)	$W_{C1/2}$ (°C)	X_c (%)
UHMWPE	146.5	118.8	9.1	51.6
UHMWPE/ PEG (100/3)	137.1	118.9	8.4	43.2
UHMWPE/PEG/ MAPE (100/3/3)	137.1	119.0	8.1	44.5

The mild growing trend is commonly considered as strain hardening effect. It is quite noticeable that the introduction of PEG jeopardizes the elongation at break of UHMWPE, from 640% to 560%, but involving MAPE enables the blends to possess a much higher value (760%). This is explainable as during the stretching process, the molecular chains of UHMWPE will shift against each other until it breaks. Although PEG can disentangle the twisted chain segments of UHMWPE, the defects it brings about cause faster breaks within UHMWPE/PEG blends. As MAPE connects PEG and UHMWPE, the more integrated structure is capable of withstanding higher deformation, and thus the ternary blends own greater value of elongation at break.

Thermal Properties of UHMWPE Blends

This research also studied the thermal stability and the heat resistance of the blends as a reference to the utilization of the material. Vicat softening temperature (VST) of UHMWPE and its blends were tested, and the results are listed in Figure 8.

VST, an important indicator that characterizes heat resistance, is the determination of the softening point for materials that have no definite melting point, such as plastics. From Figure 8, it can be seen that the VST of pure UHMWPE is around 80.4°C, and adding a small amount of PEG does not change this figure much, which is in accordance with other findings that previously reported.[32] It is particularly noticeable that incorporating MAPE surprisingly improves the VST of UHMWPE blends, with the figure rising to ~85.7°C. The increased VST represents better dimensional stability of the material under certain heating environment, and also it means the product possesses greater rigidity and can resist deformation at higher operating temperature.[38–40]

On the other hand, regarding thermal stability, TGA tests were conducted for three different groups, and the results are shown in Figure 9. According to this figure, adding PEG and MAPE does not largely change the degradation process of virgin UHMWPE. However, there are indeed some slight differences occurred between 350°C and 450°C, and the detailed data is listed in Table II. The initial decomposition temperature of virgin UHMWPE is slightly improved by adding PEG, with the figure increasing from 419.4°C to 426.5°C, while further introducing MAPE barely enhances the $T_{5\%}$ of UHMWPE/PEG blends. In terms of the peak decomposition temperature, these three groups do not show any obvious variation. Hence, although the initial decomposition temperature, $T_{5\%}$, is increased slightly, incorporating a small amount of PEG and MAPE does not jeopardize nor greatly enhance the thermal stability of virgin UHMWPE. The decomposing process remains almost a same pattern.

The melting and crystallizing behavior of UHMWPE blends were characterized and tracked by DSC tests. The scanning curves are presented in Figure 10, and the corresponding data is listed in Table III.

According to Table III, the addition of PEG and MAPE reduces the T_{Mp} of virgin UHMWPE, from 146.5°C to 137.1°C. The peak melting temperature is largely dependent on the crystalline structure of a specific material, and thus this phenomenon can be speculated as introducing PEG could hinder or even damage

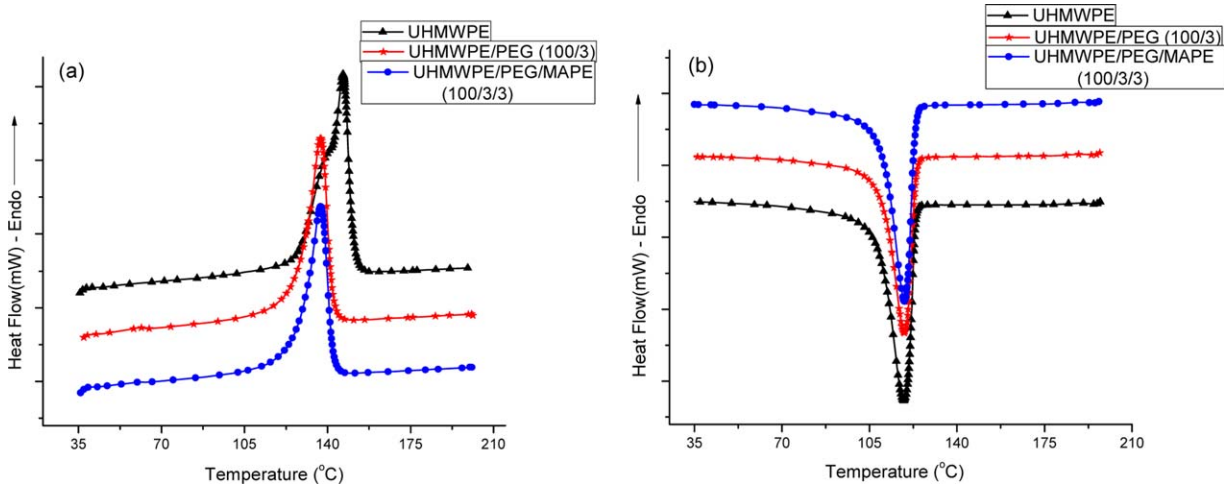

Figure 10. DSC scans of UHMWPE blends: (a) Melting curves, (b) Crystallization curves. [Color figure can be viewed in the online issue, which is available at wileyonlinelibrary.com.]

the integrity and structure of UHMWPE crystal. Concerning the crystallization parameters, incorporating PEG and MAPE presents little effects on the peak crystallization temperature (T_{Cp}), but the value of $W_{C1/2}$, which represents the crystallizing rate, is decreased, indicating faster crystallization process. These results are explainable, because foreign matter, like PEG and MAPE, could function as the centre of heterogeneous nucleation, and the UHMWPE segments will crystallize and grow along those impurities, thus facilitating the course of crystallization.[41–44] It is noticeable that the relative crystallinity of UHMWPE is decreased evidently after adding PEG and MAPE. The reduced crystallinity implies damaged integrity of UHMWPE crystals, which can also explain the decreased T_{Mp}.

CONCLUSIONS

Ternary blends of UHMWPE/PEG/MAPE were prepared by melt mixing technique in a twin screw extruder followed by compression molding and then evaluated regarding any changes in mechanical, thermal, and rheological properties.

1. The processability of UHMWPE/PEG blends is further improved by the addition of MAPE, and this ternary blends can be effectively extruded by a twin screw extruder with lower die pressure and better melt flowability than UHMWPE/PEG binary blends.
2. The flexural strength and impact strength of UHMWPE/PEG are increased by 12.0% and 6.1%, respectively, without any sacrifice in tensile strength, while the elongation at break, which reflects the toughness, is greatly improved by 35.7%.
3. Vicat softening temperature of UHMWPE/PEG blends is improved after MAPE added, with the figure rising from 81.0°C to 85.7°C. The decomposing process almost remains a same pattern by involving PEG and MAPE, indicating similar thermal stability. Furthermore, the peak melting temperature of pure UHMWPE is decreased by the addition of PEG and MAPE as a result of diminished crystallinity (up to 16.3%), and the crystallization process of UHMWPE is facilitated by PEG and MAPE.
4. Morphology analysis revealed that incorporating MAPE largely reduces the particle size of PEG in UHMWPE, and the dispersion of PEG particles is also improved. It is reasonably assumed that MAPE as a coupling agent enhances the interfacial interactions between UHMWPE and PEG, and therefore the more integrated structure of UHMWPE/PEG/MAPE blends is responsible for its better processability and improvements in other properties.

ACKNOWLEDGMENTS

The authors gratefully acknowledge Industry-University-Research Cooperative Project of Guangdong Province (2013B090200013) for financial supports.

REFERENCES

1. Ahmad, M.; Wahit, M. U.; Kadir, M. R. A.; Dahlan, K. Z. M.; Jawaid, M. *J. Polym. Eng.* **2013**, *33*, 599.
2. Okularczyk, W. *Arch. Civ. Mech. Eng.* **2004**, *1*, 167.
3. Kurtz, S. M.; Muratoglu, O. K.; Evans, M.; Edidin, A. A. *Biomaterials* **1999**, *20*, 1659.
4. Zacbarriades, A. E.; Kanamoto, T. *AIChE. Annu. Meet. Symp.* **1984**, *25*.
5. Whitehouse, C.; Liu, M. L.; Gao, P. *Polym. Eng. Sci.* **1999**, *39*, 904.
6. Jaggi, H. S.; Satapathy, B. K. *J. Polym. Res.* **2014**, *21*, 482.
7. Bateja, S. K.; Andrews, E. H. *Polym. Eng. Sci.* **1983**, *23*, 888.
8. Dumoulin, M. M.; Utracki, L. A.; Lara, J. *Polym. Eng. Sci.* **1984**, *24*, 117.
9. Kyu, T.; Vadhar, P. *J. Appl. Polym. Sci.* **1986**, *32*, 5575.
10. Vadhar, P.; Kyu, T. *Polym. Eng. Sci.* **1987**, *27*, 202.
11. Sawatari, C.; Matsuo, M. *Polymer* **1989**, *30*, 1603.
12. Tincer, T.; Coskun, M. *Polym. Eng. Sci.* **1993**, *33*, 1243.
13. Liu, G. D.; Li, H. L. *J. Appl. Polym. Sci.* **2003**, *89*, 2628.
14. Wang, X.; Li, H. L.; Jin, R. *J. Appl. Polym. Sci.* **2006**, *100*, 3498.
15. Aiello, R.; La Mantia, F. P. *Macromol. Mater. Eng.* **2001**, *286*, 176.
16. Utsumi, M.; Nagata, K.; Suzuki, M.; Mori, A.; Sakuramoto, I.; Torigoe, Y. *J. Appl. Polym. Sci.* **2003**, *87*, 1602.
17. Wang, X.; Wu, Q. Y.; Qi, Z. N. *Polym. Int.* **2003**, *52*, 1078.
18. Xie, M. J.; Li, H. L. *J. Appl. Polym. Sci.* **2008**, *108*, 3148.
19. Boscoletto, A. B.; Franco, R.; Scapin, M.; Tavan, M. *Eur. Polym. J.* **1997**, *33*, 97.
20. Liu, G. D.; Chen, Y. Z.; Li, H. L. *J. Appl. Polym. Sci.* **2004**, *94*, 977.
21. Xie, M. J.; Li, H. L. *Eur. Polym. J.* **2007**, *43*, 3480.
22. Xie, M. J.; Liu, X. L.; Li, H. L. *J. Appl. Polym. Sci.* **2006**, *100*, 1282.
23. Morawiec, J.; Pawlak, A.; Slouf, M. *Eur. Polym. J.* **2005**, *41*, 1115.
24. Bikiaris, D.; Panayiotou, C. *J. Appl. Polym. Sci.* **1998**, *70*, 1503.
25. Araujo, J. R.; Waldman, W. R.; De Paoli, M. A. *Polym. Degrad. Stab.* **2008**, *93*, 1770.
26. Liu, W.; Wang, Y. J.; Sun, Z. *J. Appl. Polym. Sci.* **2003**, *88*, 2904.
27. Qiu, W. L.; Zhang, F. R.; Endo, T.; Hirotsu, T. *Polym. Compos.* **2005**, *26*, 448.
28. Buckley, C. P.; Wu, J.; Haughie, D. W. *Biomaterials* **2006**, *28*, 3178.
29. Gai, J. G.; Li, H. L. *J. Appl. Polym. Sci.* **2007**, *106*, 3023.
30. Khasraghi, S. S.; Rezaei, M. *J. Thermoplast. Compos.* **2015**, *28*, 305.
31. Lim, K. L. K.; Ishak, Z. A. M.; Ishiaku, U. S.; Fuad, A. M. Y.; Yusof, A. H.; Czigany, T.; Pukanszky, B.; Ogunniyi, D. S. *J. Appl. Polym. Sci.* **2005**, *97*, 413.
32. Xie, M. J. Material Science, Ph.D. Thesis, Sichuan University, China, **2008**.
33. Petchwattana, N.; Covavisaruch, S.; Chanakul, S. *J. Polym. Res.* **2012**, *19*, 9921.

34. Wang, Q. F.; Qi, R. R.; Shen, Y. H. *J. Appl. Polym. Sci.* **2007**, *106*, 3220.

35. Coiai, S.; Passaglia, E.; Hermann, A. *Polym. Compos.* **2010**, *31*, 744.

36. Pruitt, L. A. *Biomaterials* **2005**, *26*, 905.

37. Wang, X. D.; Li, H. Q.; Jin, R. G. *J. Appl. Polym. Sci.* **2006**, *100*, 3498.

38. Li, L. J.; He, B. B.; Chen, X. *J. Appl. Polym. Sci.* **2007**, *106*, 3610.

39. Namhata, S. P.; Santolini, L.; Locati, G. *Polym. Test.* **1990**, *9*, 75.

40. Zhang, X. J.; Shen, J. C.; Yang, H. J.; Lin, Z. D.; Tan, S. Z. *J. Thermoplast. Compos.* **2011**, *24*, 735.

41. Kuznetsov, V. A.; Okhrimenko, T. M.; Rak, M. *J. Cryst. Growth* **1998**, *193*, 164.

42. Rauls, M.; Bartosch, K.; Kind, M.; Kuch, S.; Lacmann, R.; Mersmann, A. *J. Cryst. Growth* **2000**, *213*, 116.

43. Snell, E. H.; Judge, R. A.; Crawford, L.; Forsythe, E. L.; Pusey, M. L.; Sportiello, M.; Todd, P.; Bellamy, H.; Lovelace, J.; Cassanto, J. M. *Cryst. Growth. Des.* **2001**, *1*, 151.

44. Toda, A. *J. Phys. Soc. Jpn.* **1986**, *55*, 3419.